DOI: 10.54254/2755-2721/10/20230151

Modeling of neodymium-doped wideband fiber amplifier gain spectrum and numerical simulation optimization based on Matlab genetic algorithm: 1300-1400 nm peak gain maximization

Yuanjun Lu

School of Physics and Telecommunication Engineering, South China Normal University, GuangZhou, GuangDong, 510006, China

20202332011@m.scnu.edu.cn

Abstract. The gain spectrum of the neodymium-doped wideband fiber amplifier was modeled and simulated by Matlab, and the intelligent optimization algorithm (genetic algorithm) included in Matlab was used to optimize the fiber length and doping concentration to maximize the peak gain (find the optimal fiber length and doping concentration within the set range). According to the set signal optical wavelength range (1300 nm~1400 nm) and the corresponding neodymium ions four-level transition structure, the pump optical wavelength (800 nm) is designed and the four-level structure rate equation and power propagation equation are established, and Matlab programming calculates the change of gain with fiber length, neodymium ions doping concentration and pump optical power. According to the obtained gain curve, it can be inferred that under the parameter range set in this study, the gain of the neodymium-doped fiber amplifier increases significantly with fiber length and neodymium ions doping concentration, while the pump optical power has almost no effect on the gain value.

Keywords: fiber amplifier, genetic algorithms, neodymium ions.

1. Introduction

Due to the urgent need for communication, the development of erbium-doped fiber amplifiers in the nineties of the 20th century was very rapid. In 1986, David Payne's team at the University of Southampton, England, announced the invention of the first erbium-doped fiber amplifier (EDFA) [1]. Since then, the optical fiber amplifier developed by using optical fiber doped with rare earth elements has brought revolutionary changes to the field of lightwave technology. Neodymium-doped broadband fiber amplifier (NDFA) is one of them, in 1964, C. Koester and E. Snitzer of the American optical company first proposed the idea of a doped fiber amplifier and found that the addition of rare earth element neodymium in optical fiber can achieve optical amplification [2].

Due to the four-level system of neodymium ions, it is not only easy to obtain laser output but also has an absorption band and emission band in the ultraviolet to near-infrared spectral range [3]. Neodymium-doped fiber amplifiers do not have the same serious stimulated absorption phenomenon as doped bait and ytterbium fiber amplifiers and also have the advantages of low pump threshold [4], low noise figure [4], and high doping concentration [5]. Neodymium-doped fiber amplifiers have strong

DOI: 10.54254/2755-2721/10/20230151

excited state absorption in the 1300 nm band [6], limiting their applications for communication in this band, and it is important to find ways to weaken this limitation [7].

Researchers from the Lawrence Livermore National Laboratory (LLNL) could double the informational capacity of fibre-optic cables by developing a new type of fibre-optic amplifier. LLNL's new amplifier design is based on a novel neodymium-doped micro structured fiber that has been customized to preferentially enhance the optical signal gain in the E-band while effectively suppressing competing gains in other spectral bands [8]. This study aims to use Matlab modeling and numerical simulation optimization methods to explore what factors affect the gain of neodymium-doped fiber amplifiers in the specified band (1300 nm~1400 nm), so this paper is of major importance for the study of gain optimization of neodymium-doped fiber amplifiers.

2. Main content and steps

2.1. Four-level system structure of Nd^{3+} in the 1300 nm~1400 nm band and illustration of ESA process at 1300 nm for Nd^{3+}

With 800 nm pump light, $\boldsymbol{Nd^{3+}}$ in the ground state are excited to energy levels, shown in Figure 1 [3]. From $4_{F_{5/2}}$ to $4_{F_{3/2}}$; $4_{I_{13/2}}$ to $4_{I_{11/2}}$ and $4_{I_{11/2}}$ to $4_{I_{9/2}}$ are nonradiative transition , and there is a radiative transition between $4_{F_{3/2}}$ and $4_{I_{13/2}}$ [3].

Figure 2 is a simplified diagram of Figure 1.

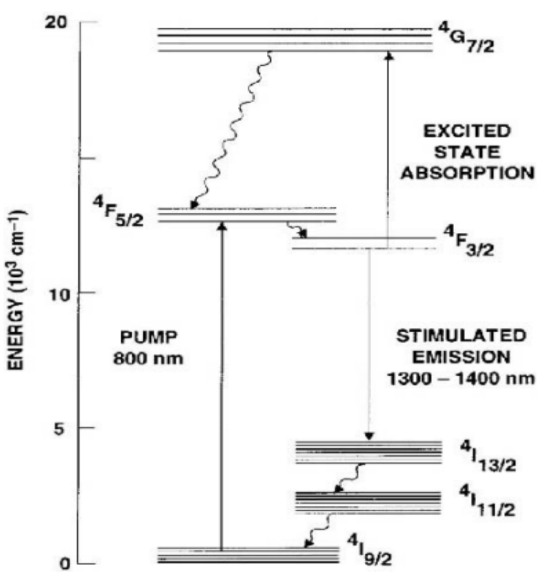

Figure 1. Illustration of ESA process at 1300 nm for Nd^{3+}[3].

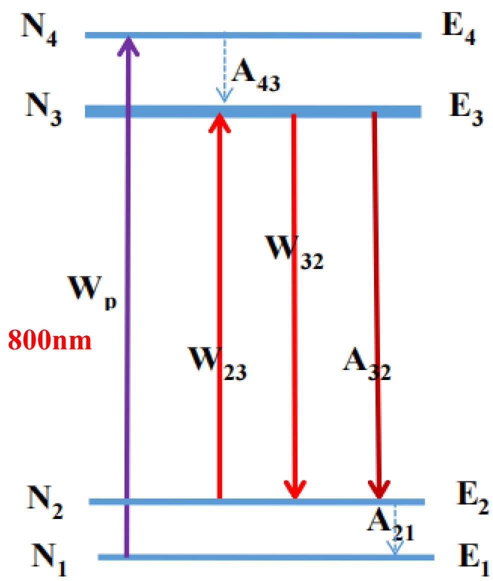

Figure 2. Simplified diagram of the four-level structure of Nd^{3+}.

The ESA (excited state absorption) process of $\boldsymbol{Nd^{3+}}$at 1300 nm means that when neodymium ions are in an excited state, they can absorb photons at 1300 nm to further excite to a highly excited state, resulting in a transition between energy levels. This process can be applied to lasers with a wavelength of 1300 nm to increase the excited state concentration of neodymium ions, thereby improving the amplification efficiency and gain of the laser [9]. At the same time, since the ESA process of neodymium ions at 1300 nm requires less excitation energy, excitation can be achieved by a small input power, thereby reducing the energy loss of the laser [3].

2.2. Four-level structure rate equation

A four-level system refers to the structure of an atomic or molecular energy level with four different energy levels, usually including ground state, metastable state, excited state, and deexcited state. Rate equations are systems of differential equations that describe the interactions between these energy levels. The rate equation of a four-level system describes the change in particle number density between the four energy levels over time and is often used to describe the energy level transition and amplification process in a laser. Its basic form is as follows [10]:

$$\frac{\partial N_1(z)}{\partial t} = -W_p(z)N_1(z) + A_{21}N_2(z) \tag{1}$$

$$\frac{\partial N_2(z)}{\partial t} = -A_{21}N_2(z) - W_{23}(z)N_2(z) + W_{32}(z)N_3(z) + A_{32}N_3(z) \tag{2}$$

$$\frac{\partial N_3(z)}{\partial t} = W_{23}(z)N_2(z) - W_{32}(z)N_3(z) - A_{32}N_3(z) + A_{43}N_4(z) \tag{3}$$

$$\frac{\partial N_4(z)}{\partial t} = W_p(z)N_1(z) - A_{43}N_4(z) \tag{4}$$

$$N = N_1 + N_2 + N_3 + N_4 \tag{5}$$

$$W_p(z) = \frac{\sigma_P P_p(z)}{h\nu_{14}A_{eff}} \tag{6}$$

$$W_{23}(z) = \frac{\sigma_{23}P_s(z)}{h\nu_{23}A_{eff}} \tag{7}$$

$$W_{32}(z) = \frac{\sigma_{32}P_s(z)}{h\nu_{32}A_{eff}} \tag{8}$$

A_{43} and A_{21} represent radiation-free transition coefficients from energy level 4 to energy level 3 and from energy level 2 to energy level 1, respectively.

A_{32}represents the rate of radiative transition from energy level 3 to energy level 2.

W_p , W_{23} and W_{32} indicate the pump light absorption rate, signal light absorption rate, and signal light stimulation emission rate.

2.3. Four-level structure power propagation equation

The change of pump power, signal power, ASE power with propagation length is called the power propagation equation [5].

$$\frac{\partial P_p(z)}{\partial z} = \Gamma_p(-\sigma_p N_1(z) - \alpha)P_p(z) \tag{9}$$

$$\frac{\partial P_s(z)}{\partial z} = \Gamma_s(\sigma_{32}N_3(z) - \sigma_{23}N_2(z) - \alpha)P_s(z) \tag{10}$$

$$\frac{\partial P_{ase}(z)}{\partial z} = \Gamma_{ase}(\sigma_{32}N_3(z) - \sigma_{23}N_2(z) - \alpha)P_s(z) + \sigma_{32}N_3(z)h\nu\Delta\nu \tag{11}$$

α and $\Delta\nu$ are the loss factor (/m) and frequency half-height full width (Hz) of the fiber material, respectively.

$$G = 10\,log_{10}\frac{P_s(z)}{P_s(0)}(dB) \tag{12}$$

Overlapping integration factor is:

$$\Gamma_{p/s/ase} = 1 - exp(-2\frac{r^2}{w^2}) \tag{13}$$

r is the radius of the fiber core (unit: m). *w* is the radius of the optical field mode field (unit: m).

$$W = r(0.65 + \frac{1.619}{V^{3/2}} + \frac{2.879}{V^6}) \tag{14}$$

V is the fiber normalized frequency.

$$V = \frac{2\pi r}{\lambda}({n_1}^2 - {n_2}^2)^{1/2} \tag{15}$$

The parameters used in equation (1)-(15) are shown in the following table.

DOI: 10.54254/2755-2721/10/20230151

Table 1. Some parameters used in the rate equation and power propagation equation of the four-level structure.

A_{32} (/s)[3]	A_{43} (/s)[3]	A_{21} (/s) [11]	σ_p (cm^2)	h (J·s)	c (/s)
543.66	2079.47	2658.8	2.05*10^-24	6.626*10^-34	3*10^8
ν_{14} (Hz)	A_{eff} (μm^2)	r (m)	V	w	α
3.75*10^14	10μm^2	1.78*10^-6	3.0756	1.2002*10^-6	0.1

2.4. Fitting of Nd^{3+} the emission section and absorption cross-section function expression in the 1300~1400 nm band

Figure 3 [3] is the emission cross-section curve of $\boldsymbol{Nd^{3+}}$ in the 1280 nm~1440 nm band, select the one pointed by the red arrow in the figure, and first use GetData (A type of data extraction software) to extract the curve data, as shown in Figure 4[3]; After extracting the data, import it into the curve fitter in Matlab, and select the function image (Figure 5) and expression (16) fitted by the Fourier series (8 terms).

$$\sigma_{32} = \begin{matrix} P0 + P1 * cos(z * k) + Q1 * sin(z * k) + P2 * cos(2 * z * k) + Q2 * sin(2 * z * k) + \\ P3 * cos(3 * z * k) + Q3 * sin(3 * z * k) + P4 * cos(4 * z * k) + Q4 * sin(4 * z * k) + \\ P5 * cos(5 * z * k) + Q5 * sin(5 * z * k) + P6 * cos(6 * z * k) + Q6 * sin(6 * z * k) + \\ P7 * cos(7 * z * k) + Q7 * sin(7 * z * k) + P8 * cos(8 * z * k) + Q8 * sin(8 * z * k) \end{matrix} \quad (16)$$

In this equation:

Table 2. The parameters resulting from the fitting function expression of σ_{32}.

P0	P1	Q1	P2	Q2	P3
2.756*10^-21	-2.407*10^-21	-7.125*10^-22	7.17*10^-22	-6.818*10^-22	-1.729*10^-22
Q3	P4	Q4	P5	Q5	P6
3.615*10^-22	-7.197*10^-23	-2.646*10^-22	6.569*10^-23	1.745*10^-22	-6.182*10^-23
Q6	P7	Q7	P8	Q8	k
-7.166*10^-24	4.338*10^-23	-2.692*10^-23	-4.401*10^-23	2.411*10^-23	0.03977

After obtaining the function expression, use equation (17) to getσ_{23}; the final result of$\sigma_{32}$and$\sigma_{23}$is shown in Figures 6 and 7.

$$\sigma_{32} = \sigma_{23}\, exp(\frac{\varepsilon_0 - h\nu}{kT}) \quad (17)$$

Table 3. The parameter used in equation (17).

Boltzmann's constant	Room temperature Thermodynamic temperature
K=1.380649*10^-23	T=298.15
velocity of light	Planck constant
c=3*10^8	h=6.626*10^-34
Zero-line energy	800 nm pump light frequency
epsilon0=1.5*10^-19	v=c/800*10^-9

DOI: 10.54254/2755-2721/10/20230151

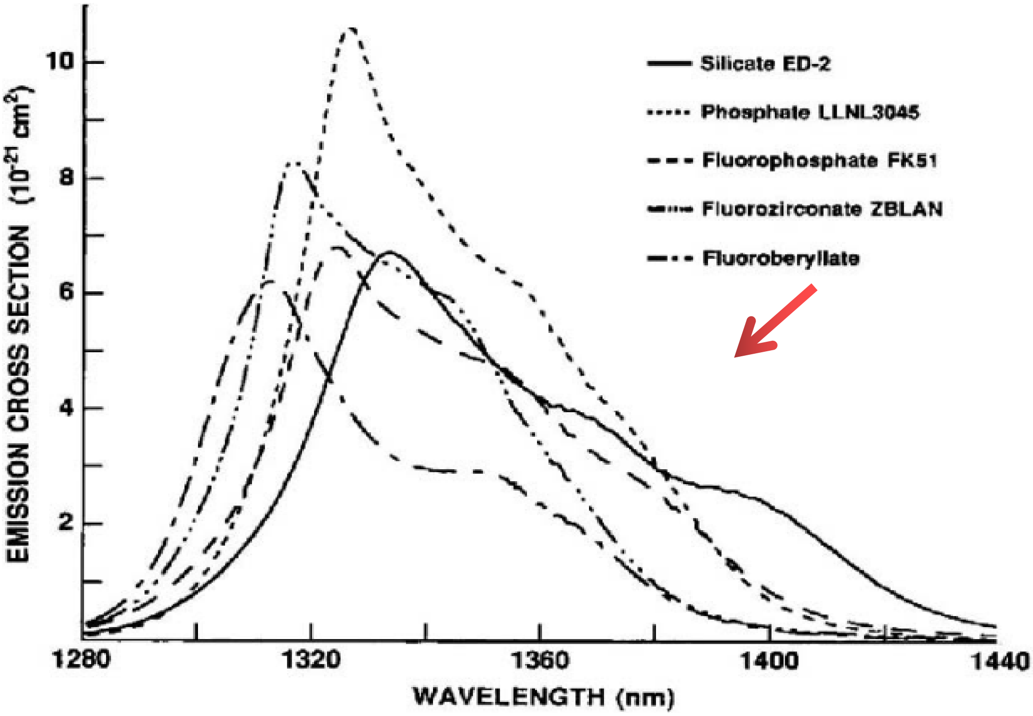

Figure 3. Emission cross-sectional curve of Nd^{3+} in the 1280 nm~1440 nm band [3].

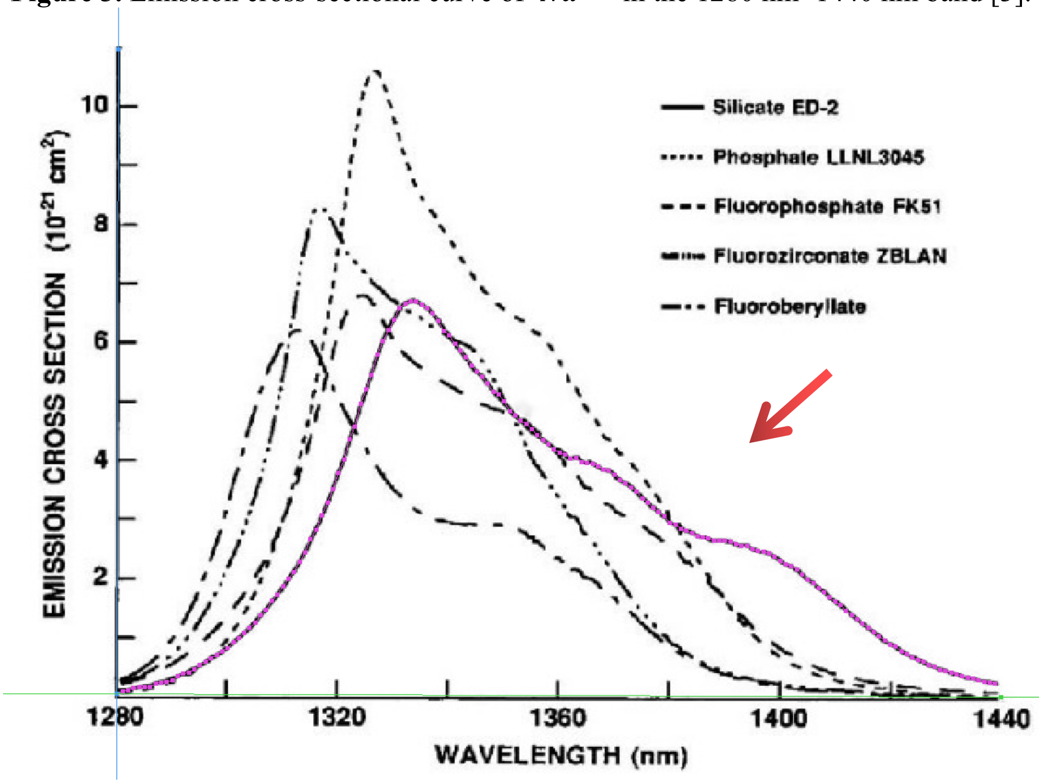

Figure 4. GetData software is used to extract specific curve renderings [3].

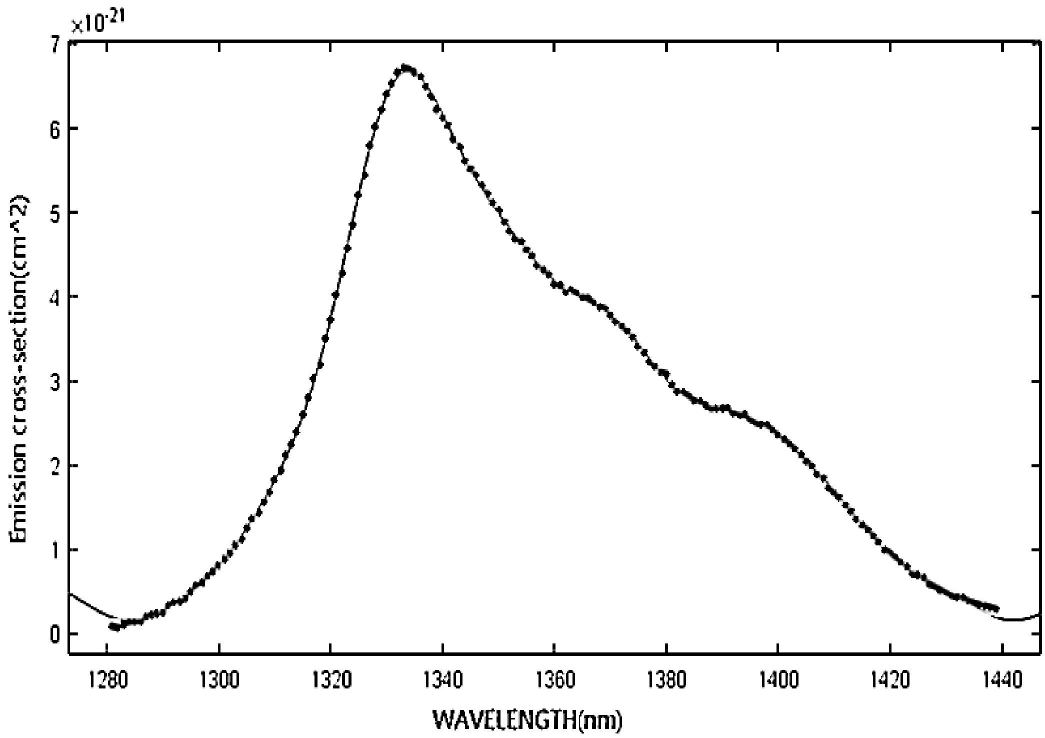

Figure 5. The function image of fitted in the curve fitter.

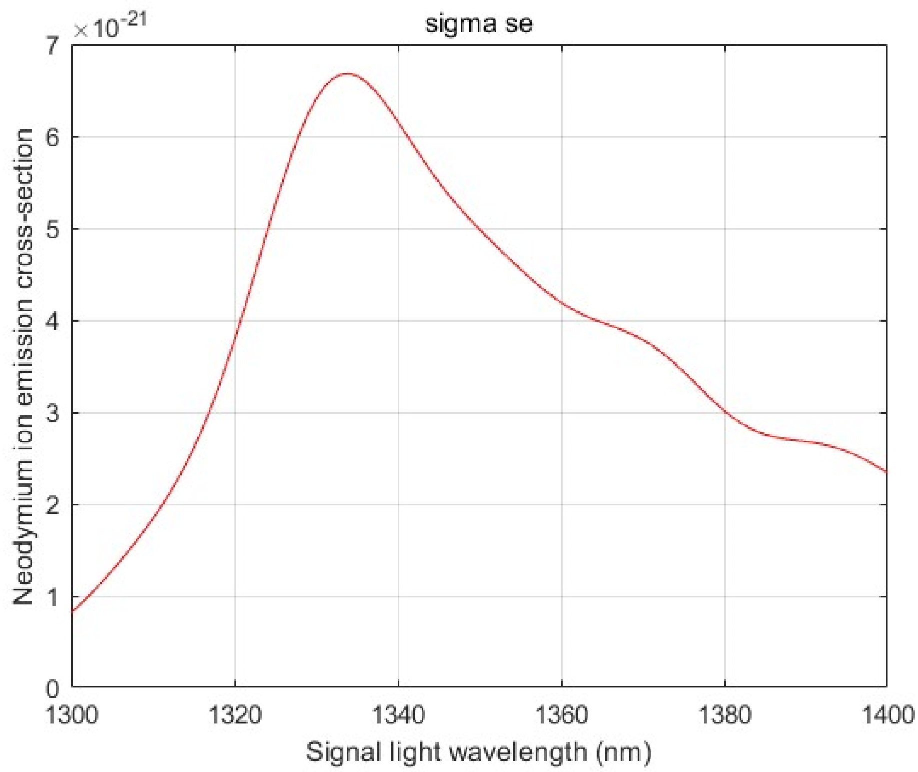

Figure 6. The function image of σ_{32}.

DOI: 10.54254/2755-2721/10/20230151

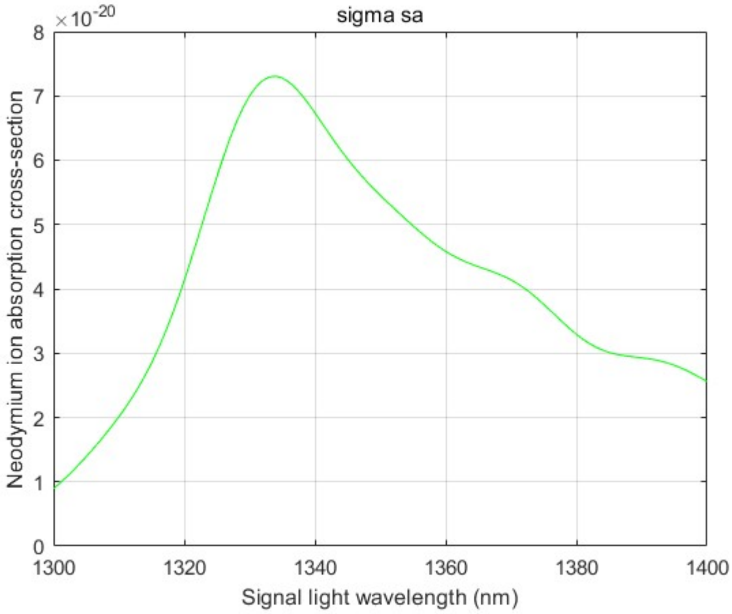

Figure 7. The function image of σ_{23}.

3. Intelligent optimization algorithm - genetic algorithm

The genetic algorithm was first proposed in the seventies of the twentieth century by Professor John Holland in the United States [12]. The algorithm mimics the evolutionary mechanisms of the biological world by drawing on Darwin's theory of evolution and Mendel's genetics, incorporating the principles of evolution and natural selection. With the research of people, it has gradually developed into a random, global, efficient, and parallel optimization algorithm [13]. This general framework for solving system optimization problems provided by genetic algorithms is widely used in function optimization, machine learning, artificial intelligence, and other fields [14].

This study uses the genetic algorithm library that comes with Matlab, which provides great convenience for solving many optimization problems (function optimization problems). The genetic algorithm in MATLAB has many characteristics, including the advantages of concise function expressions, convenient parameter setting of optimization algorithms, and so on [15].

The following is the genetic algorithm flowchart [16]:

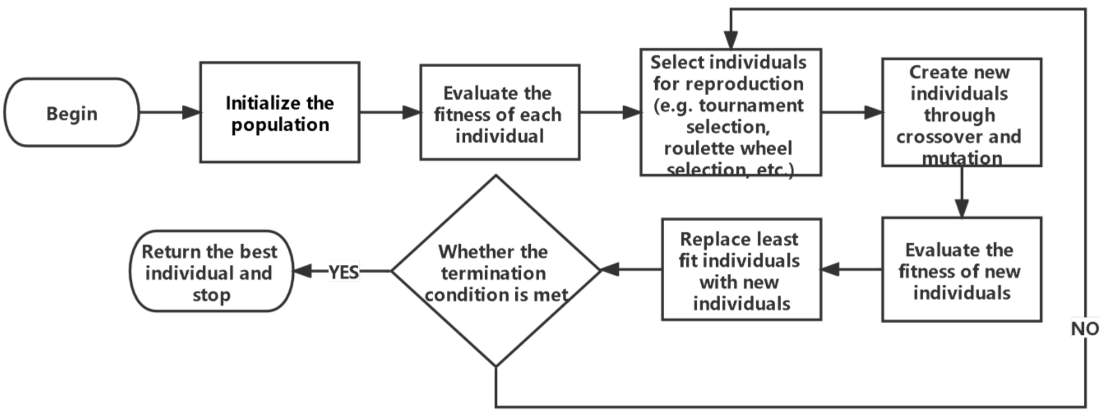

Figure 8. Flowchart of genetic algorithm.

4. Results and analysis of numerical simulation optimization

After modeling the neodymium-doped broadband fiber amplifier in Matlab using the above-mentioned neodymium ions four-level rate equation and rate propagation equation and various listed parameters, the control variable method was used to explore the effects of fiber length, neodymium ions doping concentration, and pump optical power on amplifier gain.

Figure 9 is the graph of the gain of neodymium-doped broadband fiber amplifier varies with the length of the fiber, at this time, the neodymium ions doping concentration$N = 1 \times 10^{25}$ ions$/m^3$, pump optical power=200 mW, signal optical power=1×10^{-6} Wremain unchanged, change the fiber length $L_1 = 2\,m,\ L_2 = 4\,m,\ L_3 = 6\,m,\ L_4 = 8\,m$.

It can be observed from Figure 9 that when the fiber length is a fixed value, the fiber amplifier gain increases and then decreases with the signal optical wavelength (1300 nm~1400 nm), and begins to decrease after the gain reaches a peak at about 1334 nm(43.9363 dB); When the signal light wavelength is fixed, the amplifier gain increases significantly as the fiber length increases.

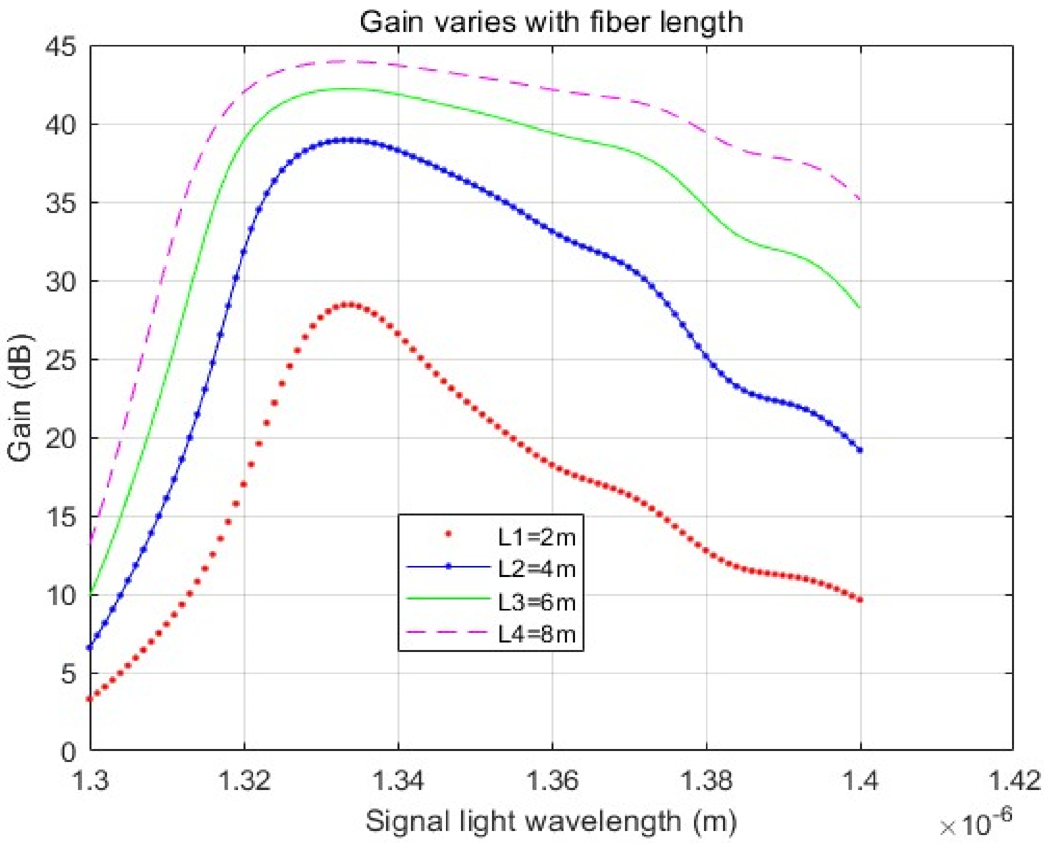

Figure 9. The gain varies with the length of the fiber.

Figure 10 is the graph of the gain of neodymium-doped broadband fiber amplifier varies with the doping concentration of neodymium ions, at this time, keep the fiber length $L = 2\,m$, pump optical power=200 mW, signal optical power=1×10^{-6} W, change the neodymium ions doping concentration $N_1 = 1 \times 10^{25}$ ions$/m^3$,$N_2 = 2 \times 10^{25}$ ions$/m^3$,$N_3 = 4 \times 10^{25}$ ions$/m^3$,$N_4 = 8 \times 10^{25}$ ions$/m^3$.

It can be observed from Figure 10 that when the neodymium ions doping concentration is a fixed value, the gain of the fiber amplifier increases and then decreases with the wavelength of signal light (1300 nm~1400 nm), and begins to decrease after the gain reaches a peak at about 1333 nm (48.552 dB); When the signal light wavelength is fixed, the amplifier gain increases significantly as the neodymium ions doping concentration increases.

DOI: 10.54254/2755-2721/10/20230151

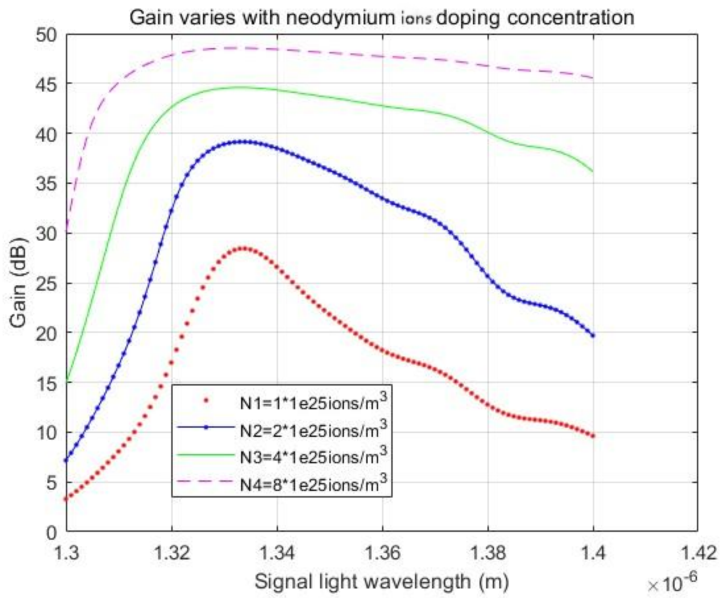

Figure 10. The gain varies with the neodymium ions doping concentration.

Figure 11 is the graph of the gain of neodymium-doped broadband fiber amplifier varies with the optical power of the pump, at this time, keep the fiber length $L = 2\ m$, $N = 1 \times 10^{25}$ ions/m^3, signal optical power=$1 \times 10^{-6}\ W$, change the pump optical power $P_{P_1} = 100\ mW$, $P_{P_2} = 200\ mW$, $P_{P_3} = 300\ mW$, $P_{P_4} = 400\ mW$.

From Figure 11, it can be observed that the pump optical power has little effect on the amplifier gain within the parameters of this study.

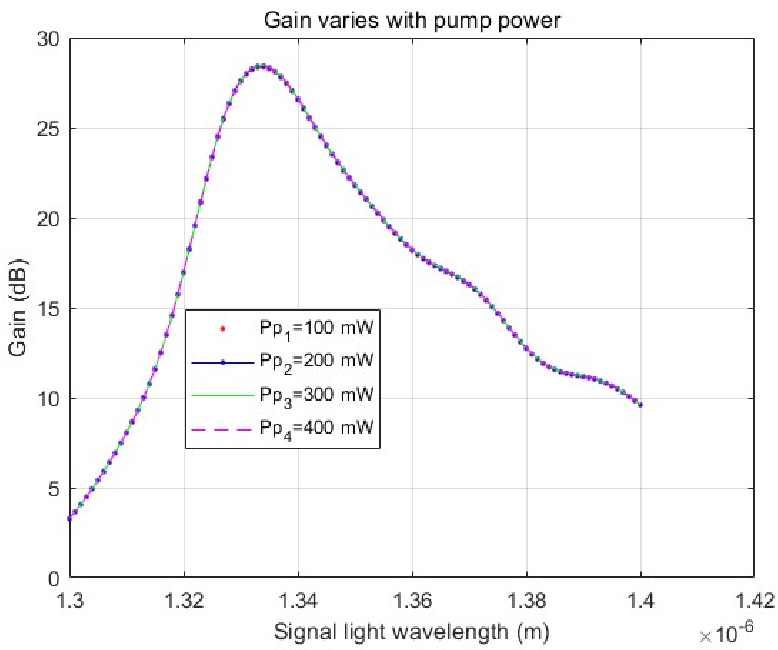

Figure 11. The gain varies with the optical power of the pump.

Figure 12 shows the optimization iteration process and result plot of the genetic algorithm. Since the genetic algorithm model in Matlab can only calculate the minimum value of the function, the objective function gain G for fitness is set to -1*G in the study, and because of the randomness of its initialized population, the optimal gain obtained each time is not necessarily the same, and about fifty runs of the optimization code are carried out in the study to select the result with the largest gain.

The results obtained here are within the parameters set by the study ($L = 1\,m \sim 8\,m$; $N = 1 \times 10^{25}$ ions/m^3~8×10^{25} ions/m^3), when $L = 7.7591\,m$, $N = 7.7211 \times 10^{25}$ ions/m^3, the fiber amplifier obtains the maximum gain, which can reach 52.2987 dB. Optimization completed: average variation of the fitness value below the options. Function Tolerance. x= 7.7277 7.7591

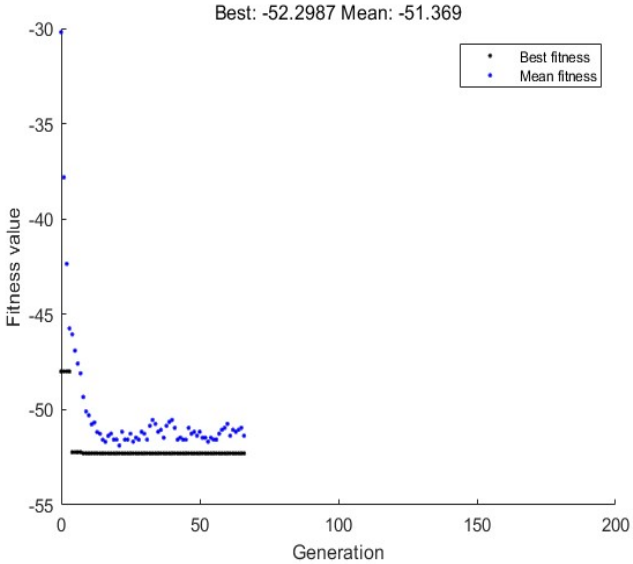

Figure 12. The genetic algorithm iteration process and the result.

5. Conclusion

This study shows that for neodymium-doped broadband fiber amplifiers, fiber length, and neodymium ion doping concentration are the main factors affecting the gain value, and the influence of pump optical power on the gain is not reflected in this study. Therefore, when studying the gain spectrum optimization of neodymium-doped broadband fiber amplifiers, the influence of fiber length and neodymium ion doping concentration should be focused on, and the influence of pump optical power on gain needs to be further studied and elucidated. At the same time, the intelligent optimization algorithm (genetic algorithm) can be used to obtain the maximum fiber length and neodymium ion doping concentration optimal value within the corresponding parameter range more quickly and accurately. However, there are many shortcomings in this study, and the four-level electron transition map of neodymium ions may be imprecise due to the simplified application of the rate and power propagation equations. The limitations of the study band and the control range of fiber length and neodymium ion doping concentration will also cause the one-sided conclusion of the study. Future research should pay more attention to the improvement of modeling accuracy and the expansion of the range of research parameters so that many factors can influence the gain of fiber amplifiers more accurately.

References

[1] Ren G J, Wei Z, Zhang Q and Yao J Q 2009 Study of Nd^{3+}-doped polarization maintaining fiber amplifier (in Chinese) Acta Phys. Sin. 58(6) pp 3897-3902 doi: 10.7498/aps.58.3897.

[2] Boley C D, Dawson J W, Kiani L S, Pax P H 2019 Mar 20 E-band neodymium-doped fiber amplifier: model and application Appl. Opt. 58(9) pp 2320-2327 doi: 10.1364/AO.58.002320. PMID: 31044936.

[3] Miniscalco W T 2001 Optical and Electronic Properties of Rare Earth Ions in Glasses.

[4] Miyazaki T, Inagaki K and Karasawa Y 1996 A high power Nd- doped double-clad fibe-r amplifier at 1.06 μm SPIE2699 pp 254-265.

DOI: 10.54254/2755-2721/10/20230151

[5] Rochat E 2000 High Power optical fiber amplifiers for coherent inter-satellite communication Universite de Neuchatel Institut de Microtechnique pp 1-113.

[6] Lumholt O, Obro M and Bjarklev A 1992 Optimum placement of filters in 1300 nm Nd-doped amplifiers Opt. Commun. 89 pp 49-51.

[7] Kong Y, Guo M X and Lu Y T 2004 Analysis of Nonlinear Refractive Index of Neodymium-Doped Fiber Amplifier[J](in Chinese) Chinese Journal of Lasers 31(7) p 4.

[8] Neodymium-Doped Fiber Amplifier and Laser | Innovation and Partnerships Office (llnl.gov).

[9] Jay W D, Leily S K, Paul H P, Graham S A, Derrek R D, Victor V K, Diana C, Nick S, Matthew J C, Robert P C and Michael J M 2017 E-band Nd3+ amplifier based on wavelength selection in an all-solid micro-structured fiber Opt. Express 25 pp 6524-6538.

[10] Kong Y, Guo M X, Lu Y T 2003 The Influence of the Fiber Amplifier Bending Loss on Fiber′s Gain ACTA PHOTONICA SINICA 32(8) pp 900.

[11] Liu J L, Wang W C, Xiao Y B, Huang S J, Mao L Y and Zhang Q Y 2019 Nd^{3+}-doped TeO_2–MoO_3–ZnO tellurite glass for a diode-pump 1.06 μm laser J. Non-Crystalline Solids 506 p 32-38 ISSN 0022-3093.

[12] Holland J H 1975 Adaptation in natural and artificial systems: an introductory analysis with applications to biology, control, and artificial intelligence[M] Ann Arbor: University of Michigan Press.

[13] Rodés J P, Pérez-Gracia V and Martínez-Reguero A 2015 Evaluation of the GPR frequency spectra in asphalt pavement assessment Constr. Build. Mater. 96 pp 181-188.

[14] Zhou Y, Hu Z G 2018 Improved fast genetic algorithm in function optimization Application Modern Electronics Technology 41(17) p 153-157.

[15] Liu G Y 2022 Application of MATLAB Genetic Algorithm in Function Optimization Problems Ship. Elec. Eng. 42(12) pp 50-53.

[16] Deng F Q, Huang H Z, Tan C E, Fu L H, Zhang J M and Lin T L 2023 Multi-robot Task Allocation Algorithm Combining Genetic Algorithm and Rolling Scheduling Comp. App. pp 1-9.